February 2002 • NREL/TP-500-29415

Technical Report

Systematic Controller Design Methodology for Variable-Speed Wind Turbines

M. Maureen Hand and Mark J. Balas

National Renewable Energy Laboratory

1617 Cole Boulevard
Golden, Colorado 80401-3393

NREL is a U.S. Department of Energy Laboratory
Operated by Midwest Research Institute • Battelle • Bechtel

Contract No. DE-AC36-99-GO10337

February 2002 • NREL/TP-500-29415

Systematic Controller Design Methodology for Variable-Speed Wind Turbines

M. Maureen Hand and Mark J. Balas

Prepared under Task No. WER2.4010

National Renewable Energy Laboratory

1617 Cole Boulevard
Golden, Colorado 80401-3393

NREL is a U.S. Department of Energy Laboratory
Operated by Midwest Research Institute • Battelle • Bechtel

Contract No. DE-AC36-99-GO10337

NOTICE

This report was prepared as an account of work sponsored by an agency of the United States government. Neither the United States government nor any agency thereof, nor any of their employees, makes any warranty, express or implied, or assumes any legal liability or responsibility for the accuracy, completeness, or usefulness of any information, apparatus, product, or process disclosed, or represents that its use would not infringe privately owned rights. Reference herein to any specific commercial product, process, or service by trade name, trademark, manufacturer, or otherwise does not necessarily constitute or imply its endorsement, recommendation, or favoring by the United States government or any agency thereof. The views and opinions of authors expressed herein do not necessarily state or reflect those of the United States government or any agency thereof.

Available electronically at http://www.osti.gov/bridge

Available for a processing fee to U.S. Department of Energy and its contractors, in paper, from:

U.S. Department of Energy
Office of Scientific and Technical Information
P.O. Box 62
Oak Ridge, TN 37831-0062
phone: 865.576.8401
fax: 865.576.5728
email: reports@adonis.osti.gov

Available for sale to the public, in paper, from:

U.S. Department of Commerce
National Technical Information Service
5285 Port Royal Road
Springfield, VA 22161
phone: 800.553.6847
fax: 703.605.6900
email: orders@ntis.fedworld.gov
online ordering: http://www.ntis.gov/ordering.htm


Printed on paper containing at least 50% wastepaper, including 20% postconsumer waste

Table of Contents

List of Tables iv
List of Figures iv
Abstract v
Introduction 1
Dynamic Modeling 2
Traditional Controller Design Methodology 4
Systematic Controller Design Methodology 6
Non-Linear Model Versus Linear Model 13
Conclusions 18
Nomenclature 19
References 20

List of Tables

Table I. Statistics Describing Wind Input Files. 6
Table II. Comparison of Performance Metrics for Non-Linear and Linear Model-Based Controller Designs 16

List of Figures

Figure 1. Torque coefficient surface as a function of tip-speed ratio and blade-pitch angle. All negative c_q values have been set to zero. 2
Figure 2. Simulation block diagram 3
Figure 3. Power coefficient surface as a function of tip-speed ratio and blade-pitch angle. All negative c_p values have been set to zero. 5
Figure 4. Example of c_P versus λ for three pitch angles 5
Figure 5. Performance metric surfaces generated using the non-linear turbine model for k_I = 1 deg/rad. 7
Figure 6. Performance metric surfaces generated using the non-linear turbine model for k_I = 5 deg/rad 8
Figure 7. Performance metric surfaces generated using the non-linear turbine model for k_I = 10 deg/rad 9
Figure 8. Time-series traces of turbine performance 11
Figure 9. Rotor speed response to step in wind input 12
Figure 10. Pitch rate response to step in wind input 13
Figure 11. Performance metric surfaces generated using the first linear model ($\omega_{T\,OP}$ = 11 rad/s; w_{OP} = 7.5 m/s; and β_{OP} = 9°) for k_I = 5 deg/rad. 14
(b) RMS speed error (rad/s) 15
Figure 12. Performance metric surfaces generated using the second linear model ($\omega_{T\,OP}$ = 11 rad/s; w_{OP} = 10 m/s; and β_{OP} = 12°) for k_I = 5 deg/rad 15
Figure 13. Regions of optimal operation 17
Figure 14. Time-series traces of turbine performance under the optimal gains as determined using each of the three models 18

Abstract

Variable-speed, horizontal axis wind turbines use blade-pitch control to meet specified objectives for three regions of operation. This paper provides a guide for controller design for the constant power production regime. A simple, rigid, non-linear turbine model was used to systematically perform trade-off studies between two performance metrics. Minimization of both the deviation of the rotor speed from the desired speed and the motion of the actuator is desired. The robust nature of the proportional-integral-derivative controller is illustrated, and optimal operating conditions are determined. Because numerous simulation runs may be completed in a short time, the relationship between the two opposing metrics is easily visualized.

Traditional controller design generally consists of linearizing a model about an operating point. This step was taken for two different operating points, and the systematic design approach was used. The surfaces generated by the systematic design approach using the two linear models are similar to those generated using the non-linear model. The gain values selected using either linear model-based design are similar to those selected using the non-linear model-based design. The linearization point selection does, however, affect the turbine performance. Inclusion of complex dynamics in the simulation may exacerbate the small differences evident in this study. Thus, knowledge of the design variation due to linearization point selection is important.

Introduction

Recently, utility-scale wind turbine manufacturers have begun to explore the possibility of operating turbines at variable rotational speeds. Because variable-speed wind turbines have the potential for increased energy capture, controller design has become an area of increasing interest. Blade-pitch regulation provides means for initiating rotation, varying rotational speed to extract power at low wind speeds, and maintaining power production at a maximum level. Controllers must be designed to meet each of these objectives, but this study pertains only to constant power production.

The power regulation regime is entered when the turbine reaches the design rotor speed for maximum power production. Under these conditions, rotational speed is constrained to a specified maximum value through blade-pitch regulation. Fluctuations in wind speed are accommodated to prevent large excursions from the desired rotational speed, which regulates rotor torque. Correspondingly, the power production is also constrained to a relatively constant level. In addition to maintaining a constant rotational speed, actuator movement must be restrained to prevent fatigue and overheating. The combination of maintaining a constant rotational speed and minimizing actuator motion are the control objectives specified for the power regulation regime.

Controller design has centered mainly on simple, linear, proportional-integral-derivative (PID) controllers, which are easily implemented in the field environment. Gain selection for these controllers has generally been a trial-and-error process relying on experience and intuition from the engineers. However, performance improvement as a result of blade-pitch control has been demonstrated (Arsudis and Bohnisch 1990, De la Salle et al. 1990, Leithead et al. 1991, Leithead et al. 1990, Stuart et al. 1996). While these studies have shown that simple controllers reduce variation about an operating point, the ultimate potential for improved performance as a result of controlling rotor speed is not quantified. Also, the PID gain selection process may result in adequate operation, but there is no information as to the potential improvement of performance with different gain values.

Although industry has embraced the PID controller, researchers have begun to investigate the capabilities of more sophisticated control designs such as state estimation designs (Bongers et al. 1989, Bossanyi 1989, Ekelund 1994, Kendall et al. 1997). The greatest advantage of state estimation over PID control is the fact that state estimator controllers can incorporate multiple inputs and multiple outputs. Issues such as reducing blade root fatigue and shaft fatigue could be included in the control objectives. However, in order to convince industry to shift toward more complicated controllers, it is necessary to compare the state estimators with PID controllers. Establishing the performance limitations of PID control through systematic design methods will provide a basis for comparison with the sophisticated controllers that potentially will offer greater benefit to the system as a whole.

This work presents a guide for selecting gain values for a PID controller that regulates rotor speed of a variable-speed wind turbine by adjusting the blade-pitch angle. The dynamic model used to describe the turbine and its operating environment is discussed. A traditional approach to PID controller gain selection is presented for comparison to the systematic methodology. The traditional approach consists of linearizing a model about an operating point. Response to step input is examined, and the gains are altered until appropriate damping behavior is observed. This approach relies heavily on trial-and-error. Because control design generally begins with a linear model, a comparison of the systematic gain selection methodology using non-linear and linear simulations provides insight to the differences introduced by linearization. The performance predictions using the systematic design methodology based on non-linear and linear models are shown.

Dynamic Modeling

A simple, rigid, non-linear turbine model developed for the purpose of controller design (Kendall et al. 1997) was used for this design study. The geometry and aerodynamic characteristics of the simulated turbine resemble those of a Grumman Windstream-33, 10-m diameter, 20-kW turbine. The National Renewable Energy Laboratory's National Wind Technology Center modified this turbine to operate at variable speeds using blade-pitch regulation. The original drivetrain, comprising a low-speed shaft, a gearbox, a high-speed shaft, and a generator, was replaced with a single, stiff, shaft and direct-drive generator. Because the drive-train compliance was reduced to that of the stiff shaft only, it has been neglected in this model.

The fundamental dynamics of this variable-speed wind turbine are captured with the following simple mathematical model:

$$J_T \dot{\omega}_T = Q_A - Q_E \qquad [1]$$

The mechanical torque necessary to turn the generator was assumed to be a constant value commanded by the generator. Because the generator moment of inertia of a direct-drive turbine is generally several orders of magnitude less than J_T, it has been neglected. The aerodynamic torque is represented by:

$$Q_A = \frac{1}{2} \rho A R c_q(\lambda, \beta) w^2 \qquad [2]$$

The torque coefficient is a highly non-linear function of tip-speed ratio and blade-pitch angle as illustrated in Figure 1. The tip-speed ratio is defined as the ratio of the blade tip speed to the prevailing wind speed. The surface presented in Figure 1 shows only positive values of c_q because the turbine operates most often in this region. These non-linear aerodynamic characteristics are implemented as a look-up table that was generated using PROPPC (Tangler 1987). This aerodynamics code uses blade-element momentum theory and empirical models that predict stalled operation and blade tip losses.

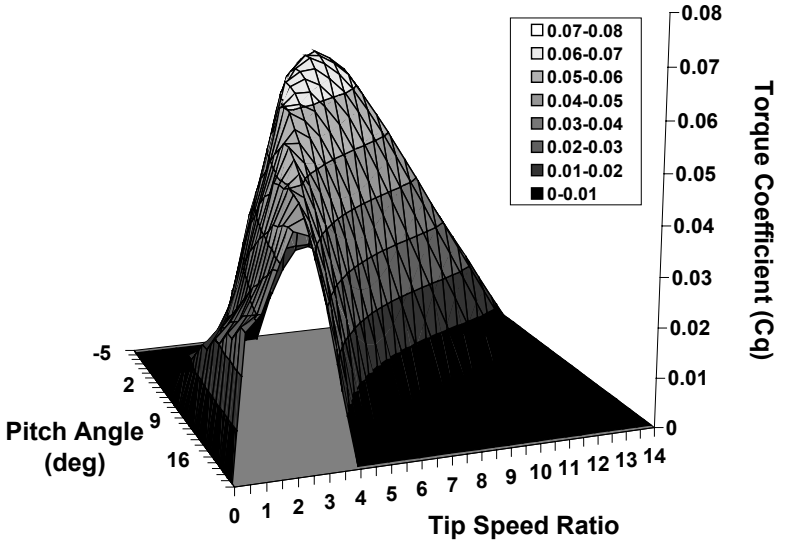

Figure 1. Torque coefficient surface as a function of tip-speed ratio and blade-pitch angle. All negative c_q values have been set to zero.

Because power limitation through speed regulation is the ultimate purpose for the controller, it is important to recognize the relationship between the power coefficient and the torque coefficient. Power extracted from the wind is shown in the following equation:

$$P = 0.5 \rho A c_P(\lambda, \beta) w^3 \quad [3]$$

Since the torque coefficient is related to the power coefficient, c_P, through the following relation

$$c_P(\lambda, \beta) = \lambda c_q(\lambda, \beta) \quad [4]$$

manipulation of the torque coefficient using λ and β will result in manipulation of the power produced by the turbine.

The block diagram in Figure 2 illustrates the simulation logic as implemented with MATLAB® Simulink® software. Actual wind data sampled at 1 Hz is the input to the non-linear plant model. The turbine speed is fed back, and the reference speed ($\omega_{T\,ref}$) is subtracted from it resulting in $\Delta\omega_T$ (noise in the sensor measurements has been neglected). This rotor-speed error is input to the controller, which commands a change in blade-pitch angle ($\Delta\beta$) based on $\Delta\omega_T$. The new pitch angle requested is then $\beta = \Delta\beta + \beta_{ref}$, which is physically limited to angles between 3° and 60°. The actuator operates on a pitch rate command. The pitch rate is determined from the difference between the commanded pitch angle and the measured blade-pitch angle (noise in the measurements is again neglected). The simulation uses a variable step size with a maximum step of 0.05 seconds. A new wind speed is read from the input file when the simulation time step corresponds to the time step of the wind data. A new rotational speed is then determined at the resulting tip-speed ratio and blade-pitch angle.

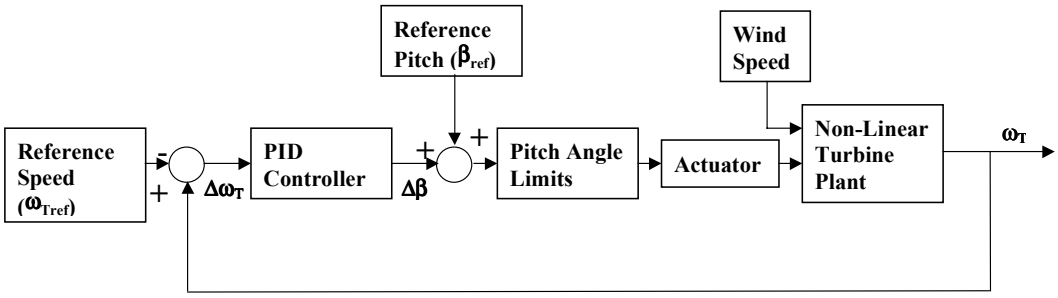

Figure 2. Simulation block diagram

Hydraulic actuators that adjust the blade-pitch angle are simulated for this study. Hydraulic fluid tends to overheat with excessive pitch motion requiring judicious use of the actuator. Additionally the linkage between the actuator and the blade-pitch mechanism may fatigue with overuse of the actuator. The pitch rate that is commanded by the actuator was physically limited to ± 10 degrees per second according to manufacturer recommendations. Another measure meant to reduce actuator motion and eliminate noise in the command signal (once it is introduced into the simulation) is the inclusion of a "dead zone" to ignore commanded pitch rates less than ± 0.1 deg/second.

To assess controller performance, two metrics were developed by Kendall et al. (1997). The root mean square (RMS) of the error between the actual rotational speed and the desired rotational speed indicates the capability of the controller to reject the wind speed fluctuations. After the simulation is completed (90

seconds), the RMS of the error is computed. The Actuator Duty Cycle (ADC) was proposed as a measure of actuator motion during a simulation run. It is simply the total number of degrees pitched over the time period of the simulation. For each simulation run, these two metrics were computed, and both must be considered in determining acceptable operating conditions.

Traditional Controller Design Methodology

A traditional approach to design of commonly used linear controllers such as proportional-integral-derivative (PID), requires that the non-linear turbine dynamics be linearized about a specified operating point. Once stability is attained, observation of the system response to step inputs provides direction in choosing gain values. This approach yields gain values that will provide adequate performance.

Linearization of the turbine eqn. [1] results in the following assuming that $Q_A|_{OP} = Q_E|_{OP}$:

$$J_T \Delta \dot{\omega}_T = \gamma \Delta \omega_T + \alpha \Delta w + \delta \Delta \beta \qquad [5]$$

where the linearization coefficients are given by:

$$\gamma = J_T \left.\frac{\partial \dot{\omega}_T}{\partial \omega_T}\right|_{OP} = \frac{1}{2}\rho A R^2 w_{OP} \left.\frac{\partial c_q}{\partial \lambda}\right|_{OP}$$

$$\alpha = J_T \left.\frac{\partial \dot{\omega}_T}{\partial w}\right|_{OP} = \frac{1}{2}\rho A R w_{OP} \left[2c_q\big|_{OP} - \lambda_{OP} \left.\frac{\partial c_q}{\partial \lambda}\right|_{OP} \right]$$

$$\delta = J_T \left.\frac{\partial \dot{\omega}_T}{\partial \beta}\right|_{OP} = \frac{1}{2}\rho A R\, w_{OP}^{\,2} \left.\frac{\partial c_q}{\partial \beta}\right|_{OP}$$

Here, $\Delta\omega_T$, Δw, and $\Delta\beta$ represent deviations from the chosen operating point, ω_{TOP}, w_{OP}, and β_{OP}.

Selection of the operating point is critical to preserving aerodynamic stability in this system. The rotational speed operating point, $\omega_{T\,OP,}$ was selected to be the desired constant speed of the turbine, 105 RPM (11 rad/s). The blade-pitch and wind speed operating points were selected using the power coefficient surface shown in Figure 3. The maximum c_p value over the entire surface occurs at a pitch angle of 3° and a tip-speed ratio of 7. Using the constant rotational speed of 11 rad/s, this tip-speed ratio corresponds to a wind speed of 7.5 m/s. At this point, the turbine would produce maximum power. However, slight deviation from this point toward negative pitch angles could result in stalled blades, which dramatically decreases the power produced. By changing the pitch angle to 9°, the magnitude of the power coefficient is reduced, but deviation around a tip-speed ratio of 7 could easily be tolerated. It is important to note that stalled blades can also occur in low tip-speed-ratio conditions.

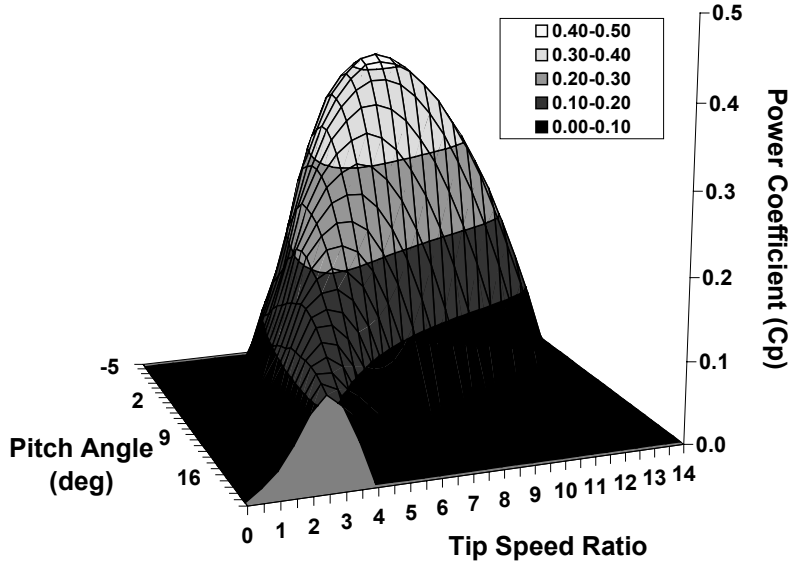

Figure 3. Power coefficient surface as a function of tip-speed ratio and blade-pitch angle. All negative c_p values have been set to zero.

Figure 4 is an example of the torque coefficient, c_q, varying with tip speed ratio, λ, for pitch angles of 3°, 9° and 12°. The peak c_q value delineates theoretically stalled and unstalled operating conditions. The region where the slope of the c_q curve is positive corresponds to stalled operating conditions. The chosen operating point of $\beta = 9°$ and $\lambda = 7$ permits deviation of the tip-speed-ratio without causing blade stall. At this point on the c_p surface, Figure 3, the power coefficient may be approximated by a relatively flat plane tangent to the surface, which is ideal for linearized models. Thus, the linearization operating point was chosen to be: $\omega_{T\,OP} = 11$ rad/s; $w_{OP} = 7.5$ m/s; and $\beta_{OP} = 9°$. The peak of the c_p surface represents the reference values used in the simulation: $\omega_{T\,ref} = 11$ rad/s; $w_{ref} = 7.5$ m/s; and $\beta_{ref} = 3°$.

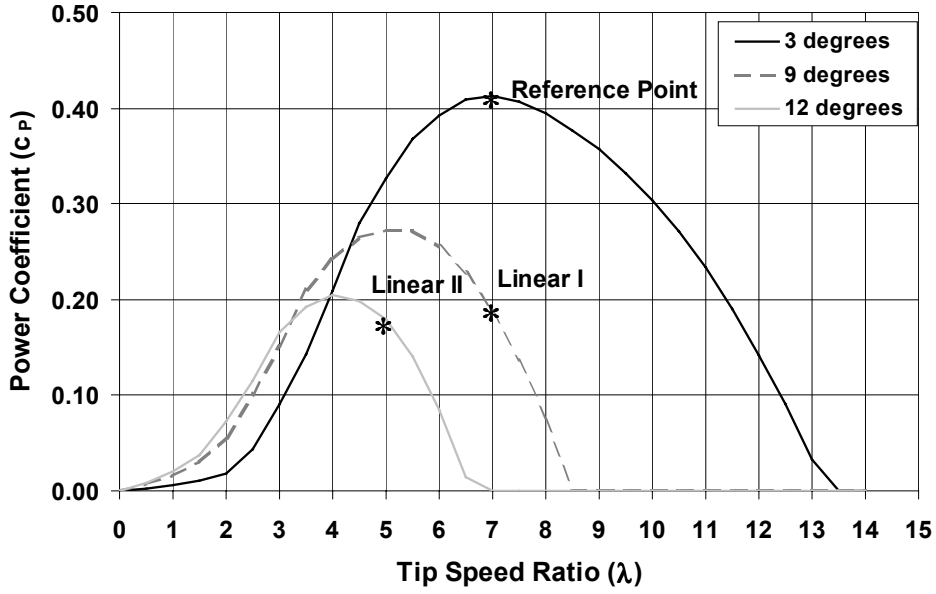

Figure 4. Example of c_P versus λ for three pitch angles

For comparison, a second operating point was selected. Simply increasing the pitch angle from 9° to 12° and maintaining the tip-speed-ratio of 7 places the point in the negative power coefficient region. By shifting the linearization point in both pitch angle and tip-speed-ratio, the tangent area around the point is maintained near the top of the curve as shown in Figure 4. This tip-speed-ratio of 5 corresponds to a wind speed of 10 m/s when maintaining the rotor speed at 11 rad/s. The second linearization point was selected to be as follows: $\omega_{T\,OP} = 11$ rad/s; $w_{OP} = 10$ m/s; and $\beta_{OP} = 12°$.

To determine regions of stable, controlled operation, the closed-loop transfer function between the output rotational speed and the reference speed is determined in the Laplace domain. The denominator of this equation is a third-order polynomial. A Routh array analysis requires each of the coefficients of the polynomial to be positive in order for the poles of the system to lie in the left-half, plane-producing stable, closed-loop operation (Hand, 1999). The gains must be as follows in order to maintain stability at the first linearization point: $k_P > -1$ deg·s/rad, $k_I > 0$ deg/rad, $k_D > -8$ deg·s^2/rad, and $(8+k_D)(1+k_P) > k_I$. For this linear approximation of the system, stability is maintained over a wide region.

At this point the designer may examine the system response to step input in order to select values for each of the gains. A step function approximates an abrupt change in wind speed and was used by Kendall et al. (1997) to tune a PI controller. Visual inspection of the rotor speed response and the pitch rate response may be used to determine the best combination of k_P and k_I gains to achieve appropriate damping of the system. However, when the third gain is introduced, this trial and error method becomes much more tedious and complicated. This method does not provide the designer with a feel for the sensitivity of the controller to slight variations in the gain values, and an optimal range of gain values is not identified.

Systematic Controller Design Methodology

In order to systematically determine combinations of three gains that produce acceptable operating conditions, the simulation was used repeatedly. Each of the gains was varied over a wide region, and the two metrics were computed for each run. Additionally, the five different wind input cases shown in Table I were used. The average value of the metrics under each combination of gains and each wind input case was computed. Contour plots for both metrics were created while the k_P and k_D gains were varied at a specific k_I. This was done for a range of k_I values from 1 to 20. Trade-off studies between the series of surfaces were performed to determine the region where optimal operating conditions exist. Lastly, time-series traces of rotational speed, pitch angle, and pitch rate for gain combinations within this region were produced to verify acceptable operation.

Table I. Statistics describing wind input files.

File Name	Mean (m/s)	Standard Deviation	RMS
Wind3	9.20	1.14	9.27
Wind4	11.43	2.28	11.66
Wind5	10.88	1.85	11.03
Medwind2	10.31	1.82	10.46
Highwind4	14.43	2.41	14.63

Figures 5-7 depict surfaces for three different values of k_I for both of the metrics. All of the contour plots indicate wide, flat surfaces for both the actuator duty cycle and the RMS of the rotational speed error. These surfaces illustrate that a wide range of gain value combinations may be chosen with similar results. Thus the controller is robust and relatively insensitive to changes in the values of the gains. However, choosing optimal operating setpoints for the gains requires closer examination of the surfaces.

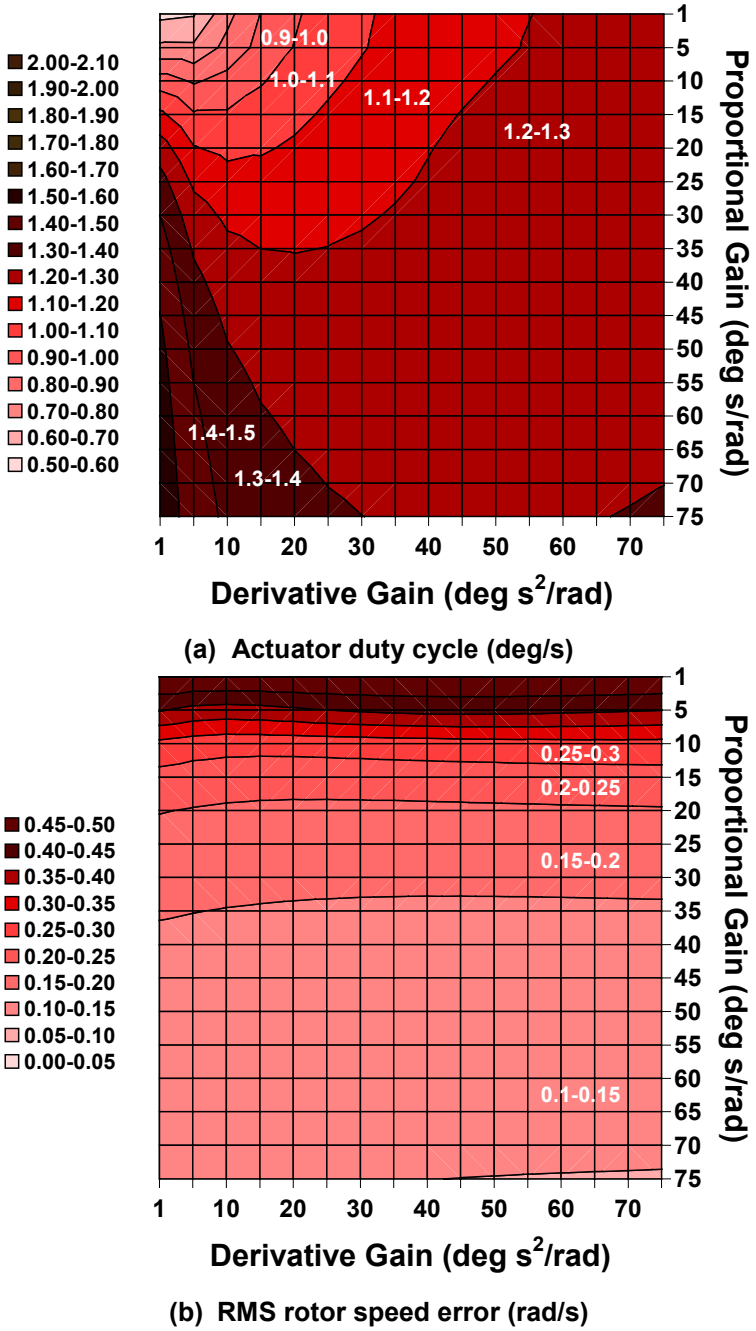

Figure 5. Performance metric surfaces generated using the non-linear turbine model for k_I = 1 deg/rad.

The actuator duty cycle surface for $k_I = 1$, Figure 5a, indicates that the mean value decreases rapidly to zero as k_P and k_D approach one. Figure 6a, which represents the surface at $k_I = 5$, portrays the opposite effect near $k_P = 1$ and $k_D = 1$, but a "bucket" with a minimum value of 0.9-1.0 deg/s appears at moderate gain values of 5-10 for both k_P and k_D. As the value of k_I is further increased to 10 in Figure 7a, the "bucket" again appears, but its minimum value of 1.0-1.1 is greater than that of the "bucket" that appears at $k_I = 5$. Therefore, the minimum value of actuator duty cycle over the entire range of the three gain values occurs somewhere between $k_I = 1$ and $k_I = 5$. The trend toward higher actuator duty cycle values as k_I increases was shown in Hand (1999) along with tables containing the simulation output values.

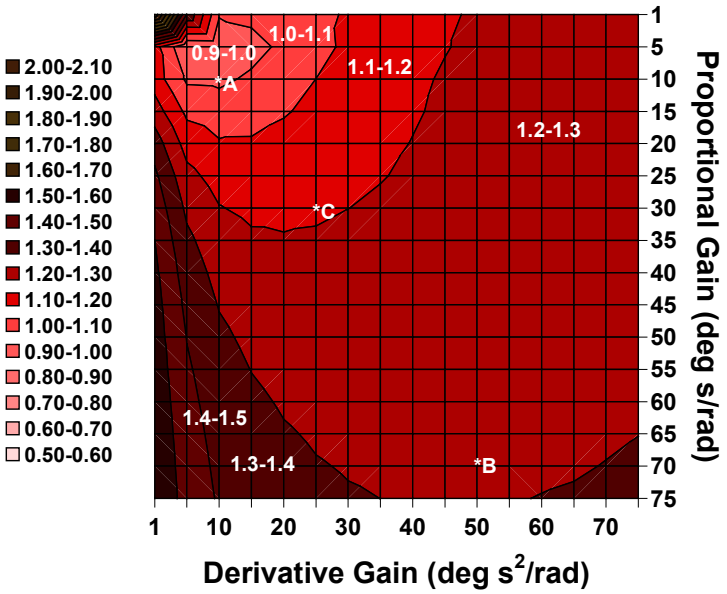

(a) Actuator duty cycle (deg/s)

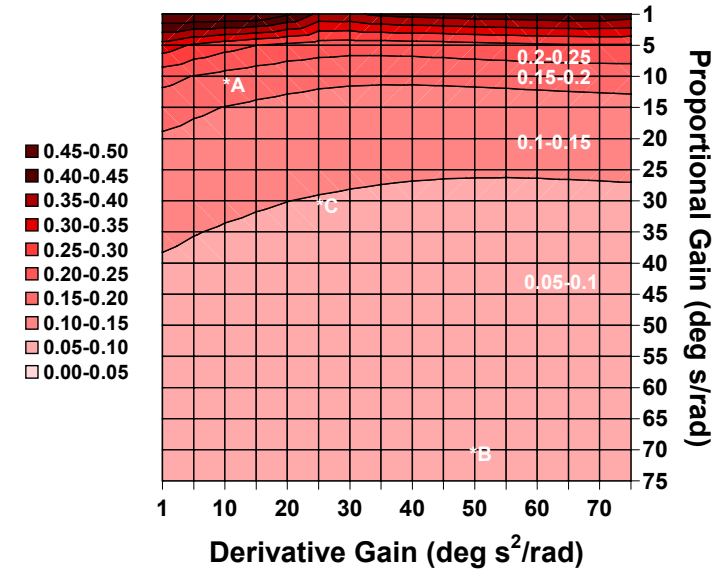

(b) RMS rotor speed error (rad/s)

Figure 6. Performance metric surfaces generated using the non-linear turbine model for $k_I = 5$ deg/rad

A similar comparison of the RMS speed error surfaces was performed to determine the location of its minimum value over the entire range of gain values. Figure 5b indicates a sharply increasing slope in the RMS speed error for $k_P < 20$. As the integral gain, k_I, increases from 1 to 5 in Figure 6b, this sharp slope boundary decreases to $k_P < 7$. Increasing the integral gain to 10, Figure 7b, moves the slope increase to $k_P < 5$. The RMS speed error slowly decreases as k_P increases such that the minimum value would occur beyond the range of the plot. However, for $k_I = 5$ to 10, the surface flattens to a mean RMS speed error of 0.05-0.10. Thus changing the value of k_I alters the point of sharply increasing slope as the proportional gain is reduced, but the flat region from which the sloped area originates is maintained.

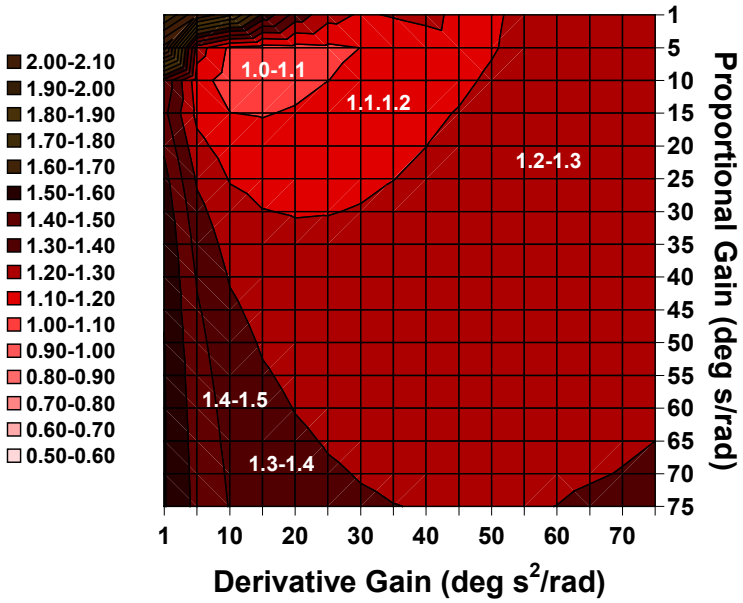

(a) Actuator duty cycle (deg/s)

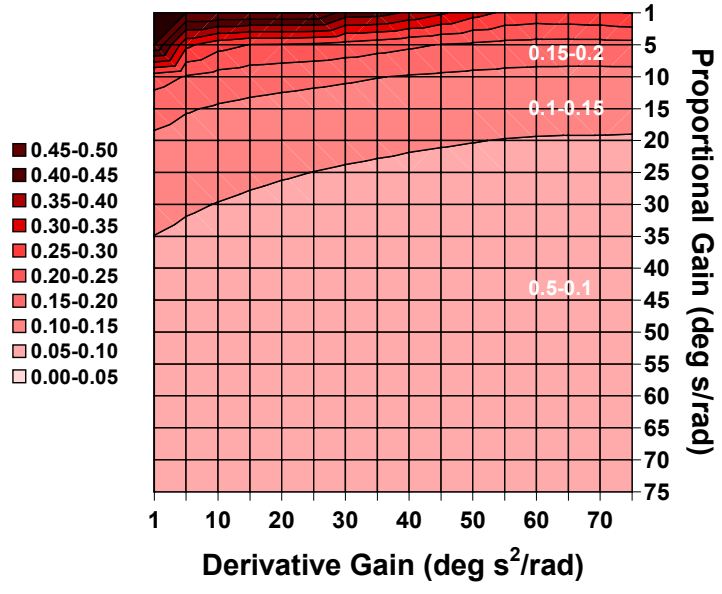

(b) RMS rotor speed error (rad/s)

Figure 7. Performance metric surfaces generated using the non-linear turbine model for $k_I = 10$ deg/rad

Both the RMS speed error and the actuator duty cycle must be considered in choosing the optimal operating conditions. If the integral gain were reduced from a value of 5, the RMS speed error surface would retain similar characteristics, but the boundary of increasing slope would begin to move from k_P = 7 towards k_P = 20. The actuator duty cycle surface would also retain similar characteristics, but the sharp rise as k_P and k_D approach one would begin to drop toward zero. The "bucket" would remain in approximately the same location. Thus, reducing k_I from 5 has little effect on the actuator duty cycle in the region of the "bucket," but the corresponding RMS speed error in that region increases. However, if the integral gain were increased, the "bucket" would begin to rise. Therefore, in order to minimize the RMS speed error and the actuator duty cycle simultaneously, the integral gain should be set at 5.

Using an integral gain of 5, the minimum actuator duty cycle region, 0.9-1.0 deg/s corresponds to an RMS speed error range of 0.15-0.20 rad/s. The point A on Figure 6a and 6b represents operating conditions where the actuator duty cycle is minimized (k_P = 10, k_I = 5, k_D = 10). An example of operation in the lowest RMS speed error range uses the operating condition at Point B (k_P = 70, k_I = 5, k_D = 50) shown on Figure 7a and 7b. Because the RMS speed error slowly decreases as the proportional and derivative gains are increased, this point also indicates operation in the low end of the lowest RMS speed error contour.

To determine which metric is more important, time-series traces of rotor speed, blade-pitch angle, and pitch rate are presented in Figure 8. The step-like nature of the pitch rate time trace originates from the different time step between the wind input file (1 Hz) and the simulation (variable time step). This creates a high frequency component of the time trace as the simulation causes the turbine reaction before the next wind input. The performance is shown for three different gain combinations based on the surfaces shown in Figure 6. The wind input for each simulation represents the highest average wind speed used in this study that produces the most extreme conditions. Figure 8a includes the time-series of the wind input.

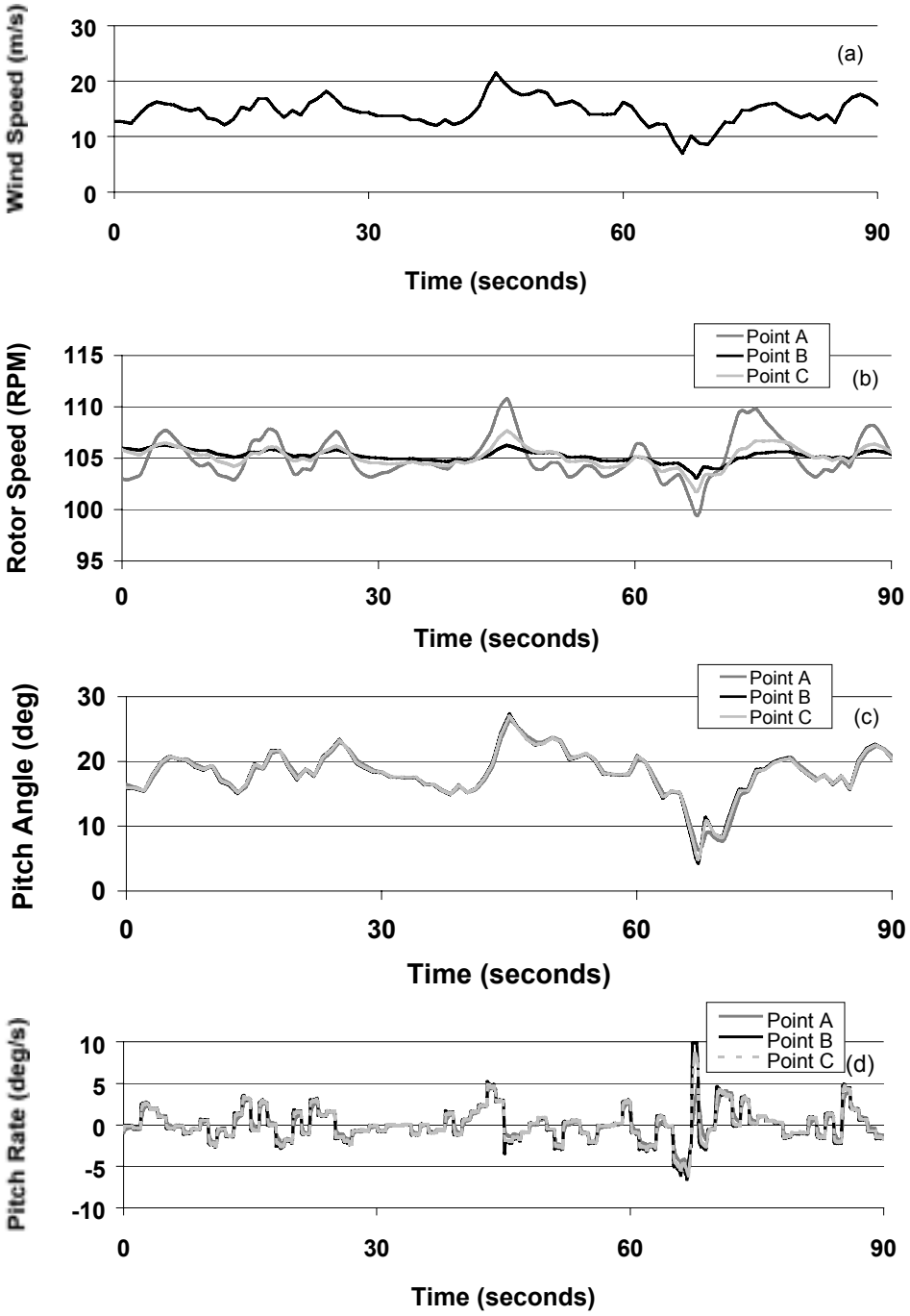

Figure 8. Time-series traces of turbine performance

Operation at Point A represents the trade-off between minimum actuator duty cycle and a higher level of RMS speed error. The rotational speed deviation from the desired 105 RPM, shown in Figure 8b, is slightly greater than ±5 RPM. The pitch rate, illustrated in Figure 8d, does not exceed ±5 deg/s. In this case the goal of maintaining constant rotational speed is not met satisfactorily. Operation at Point B depicts the trade-off between minimum RMS speed error and a higher level of actuator duty cycle. In this case the rotational speed deviation from the reference is less than ±2 RPM, and the pitch rate reaches the

limit of 10 deg/s. The pitch rate also indicates excessive motion at approximately 45 seconds. This type of motion is unacceptable when attempting to reduce fatigue and the potential for overheating.

Point C ($k_P = 30$, $k_I = 5$, $k_D = 20$) was chosen at the intersection of the minimum RMS speed error range and the lowest corresponding actuator duty cycle. The rotational speed, pitch angle, and pitch rate obtained at this operating point are included in Figure 8. The rotational speed closely tracks the desired 105 RPM throughout the simulation with peak deviations of less than ±3 RPM. The actuator duty cycle does not reach the limit, and the curve is smoother than that produced at the gain combination of Point B. Operation within this region results in the best possible combination of the two performance metrics. Figure 8c indicates that the pitch angle commanded by the controller is not noticeably affected by the choice of gain values.

When using a traditional design methodology, the engineer would subject the system to step inputs and examine the response in order to adjust the gain values. In this case of the variable-speed turbine, one would presume that the rotor speed response should be overdamped and have a short settling time on the order of less than 5 seconds. In other words, the turbine should respond quickly to wind gusts, and the rotor speed should return to the desired speed without dropping below the stated value. The pitch rate response would also be expected to respond in an overdamped manner to reduce unnecessary motion as the speed returned to its constant value. Again, a quick response (< 5 seconds) seems appropriate.

The non-linear turbine model was subjected to wind gusts simulated with step inputs while the gain values reflected those of each of the three points selected above. The rotor speed responses are shown in Figure 9 and differ from the response predicted above. The time required to return to a constant speed is lengthy, 25 seconds when the gains were in the optimal region. At Point A, the lowest actuator duty cycle region, the rotor response, is under-damped, dropping below the constant speed while the response is over-damped, as suspected, at Points B and C. The pitch rate responses are shown in Figure 10. At Point A, the pitch rate nearly reaches the limit and then slowly drops back to a stationary point. Point B, on the other hand, produces a pitch rate that nearly reaches the limit, and then becomes negative before returning to zero. At Point C, the optimal gain combination, the pitch rate jumps almost immediately to just below the rate limit and then drops almost as quickly back to zero.

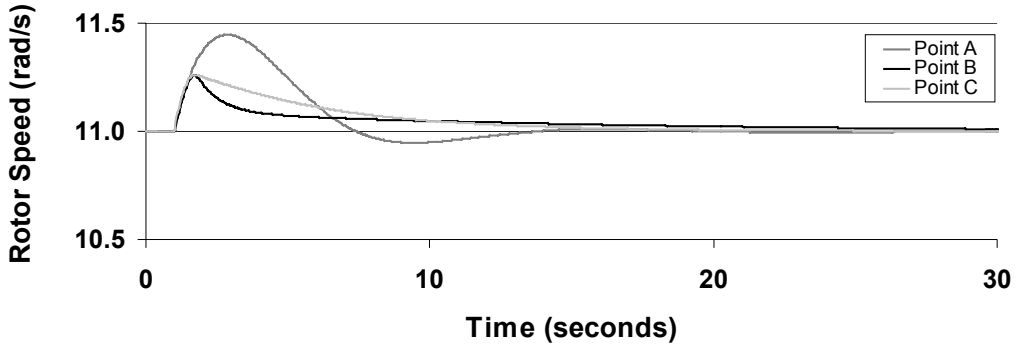

Figure 9. Rotor speed response to step in wind input

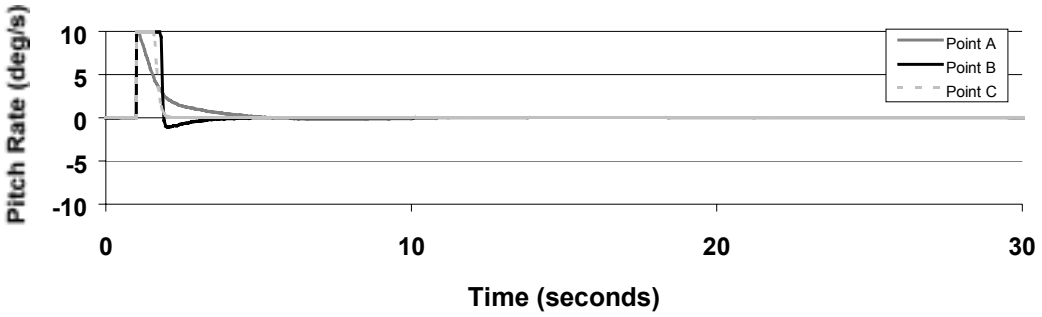

Figure 10. Pitch rate response to step in wind input

If one were designing this controller in a traditional manner, it is conceivable that none of these gain combinations would be selected. The long settling time evident in the rotor speed response seems contradictory, and the extreme amplitude of the pitch rate is surprising. However, because the wind actually behaves as a persistent disturbance, instead of a single step, the traditional interpretation of acceptable PID controller performance is questionable.

Non-Linear Model Versus Linear Model

Controller design theory is based heavily on the assumption that a linear model of a system will closely approximate the non-linear behavior observed in reality. Because the initial action a control engineer takes is to linearize the system about a chosen operating point, it is useful to explore the consequences of such action through comparison with a non-linear model. The systematic design approach described above was applied to surfaces created using two linear turbine models for comparison with those generated by the non-linear model. The linearized models described above were inserted into the Simulink® model, and the gains were varied. The results from the five wind input cases were averaged to produce each point on the surface. Surfaces depicting both the actuator duty cycle and RMS speed error were created.

Again, the $k_I = 5$ surface provided the best simultaneous minimization of both metrics. Points A, B, and C were selected in the same manner as for the surfaces generated by the non-linear turbine model. The surfaces for the Linear I and the Linear II models are shown in Figures 11 and 12 respectively.

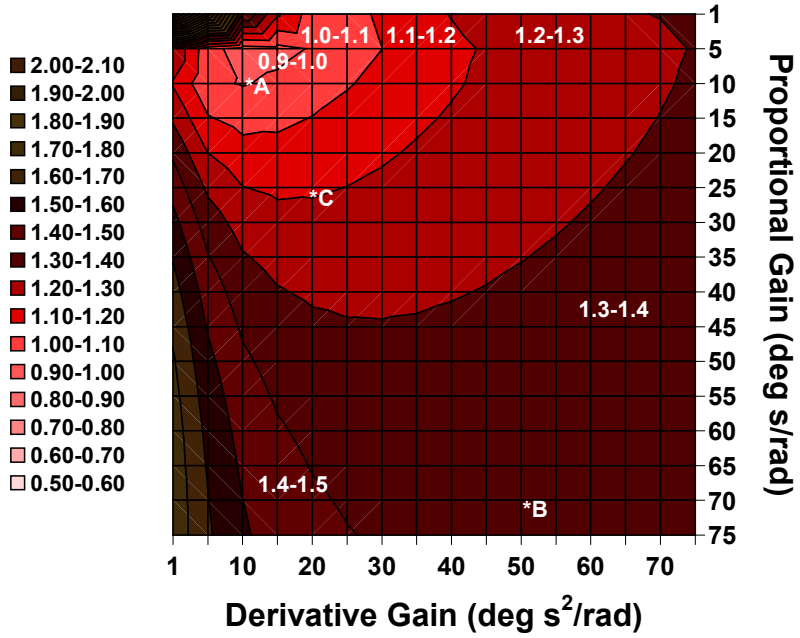

(a) Actuator duty cycle (deg/s)

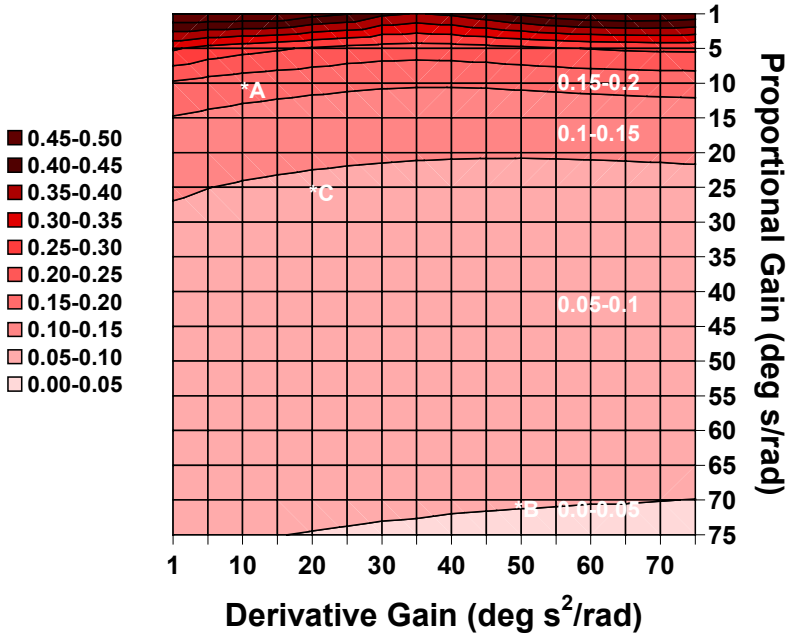

(b) RMS speed error (rad/s)

Figure 11. Performance metric surfaces generated using the first linear model ($\omega_{T\,OP}$ = 11 rad/s; w_{OP} = 7.5 m/s; and β_{OP} = 9°) for k_I = 5 deg/rad.

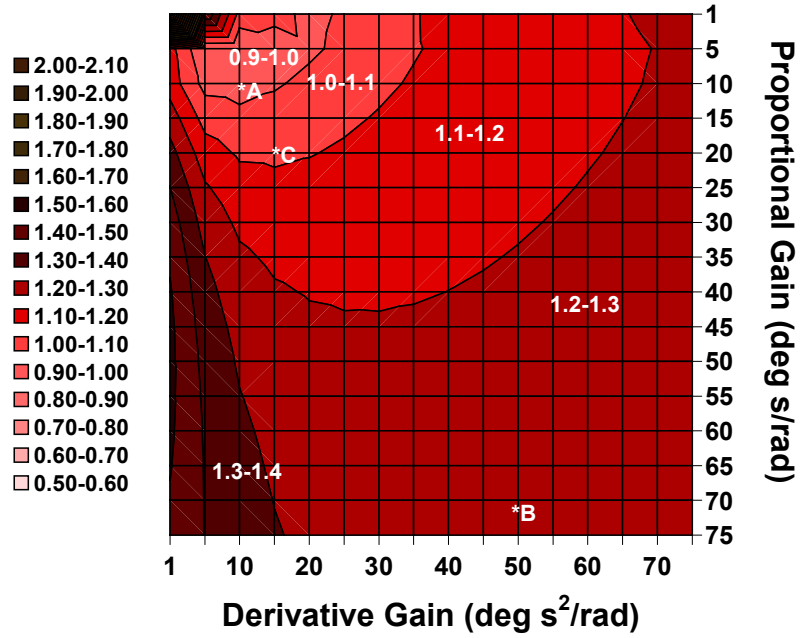

(a) Actuator duty cycle (deg/s)

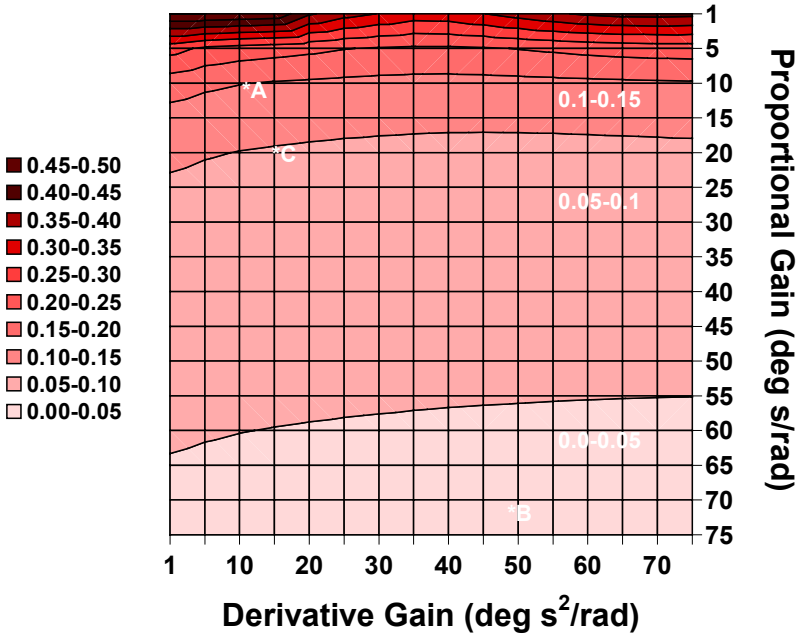

(b) RMS speed error (rad/s)

Figure 12. Performance metric surfaces generated using the second linear model ($\omega_{T\,OP}$ = 11 rad/s; w_{OP} = 10 m/s; and β_{OP} = 12°) for k_I = 5 deg/rad

In general, the surfaces created by all three models are similar. The second linear model surfaces more closely represent those generated by the non-linear model. The actuator duty cycle increases toward the perimeters of the surface most rapidly when the first linear model is used, and the corresponding non-linear model based surface is the flattest. Comparison of the RMS speed error surfaces indicates that the

non-linear model generated surface is the flattest, and the second linear model surfaces are the steepest. Thus, in the area surrounding Point C, the models all behave similarly. The greatest differences appear toward the edges of the surfaces.

The magnitudes of the metrics as well as the gain values are identical between the two models for Point A as shown in Table II. The additional contour that appears in the RMS speed error surface generated by the linear model would alter the selection of Point B slightly. A proportional gain greater than 70 would place the point in the lowest RMS speed error contour. Also, the compromise point, C, must be based on the second lowest RMS speed error contour due to the additional contour that results from use of the linear model. The intersection of the second lowest RMS speed error contour and the corresponding actuator duty cycle contour are in a slightly different location than the corresponding point on the non-linear model generated surface. This leads to slightly different gain values in this region of optimal operation.

Table II. Comparison of Performance Metrics for Non-Linear and Linear Model-Based Controller Designs

Non-Linear Model Design	**Actuator Duty Cycle (deg/s)**	**RMS Speed Error (rad/s)**
Point A $k_P = 10, k_I = 5, k_D = 10$	0.9-1.0	0.10-0.15
Point B $k_P = 70, k_I = 5, k_D = 50$	1.2-1.3	0.05-0.10
Point C *$k_P = 30, k_I = 5, k_D = 25$*	*1.1-1.2*	*0.05-0.10*
Linear I: $\omega_{T\,OP} = 11$ rad/s; $w_{OP} = 7.5$ m/s; and $\beta_{OP} = 9°$		
Point A $k_P = 10, k_I = 5, k_D = 10$	0.9-1.0	0.15-0.20
Point B $k_P = 75, k_I = 5, k_D = 50$	1.3-1.4	0.00-0.05
Point C *$k_P = 25, k_I = 5, k_D = 20$*	*1.1-1.2*	*0.05-0.10*
Linear II: $\omega_{T\,OP} = 11$ rad/s; $w_{OP} = 10$ m/s; and $\beta_{OP} = 12°$		
Point A $k_P = 10, k_I = 5, k_D = 10$	0.9-1.0	0.15-0.20
Point B $k_P = 75, k_I = 5, k_D = 50$	1.2-1.3	0.00-0.05
Point C *$k_P = 20, k_I = 5, k_D = 15$*	*1.0-1.1*	*0.05-0.10*

Comparison of the regions of optimal operation selected using the non-linear model, and the two linear models is shown in Figure 13. The optimal region selected using the second linear model deviates the most from that obtained using the non-linear model. Assuming that the non-linear model provides the best representation of actual turbine operation, time-series traces were created using the optimal gain combination obtained from both linear models. Figure 14 illustrates the time-series turbine behavior when subjected to the most extreme wind speed case. Included in Figure 14 are the time traces produced by the non-linear plant simulation when the gains are chosen using the non-linear model design approach.

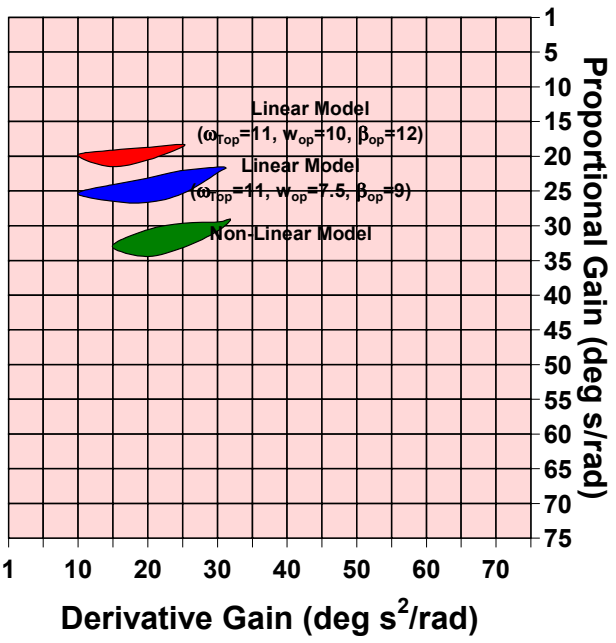

Figure 13. Regions of optimal operation

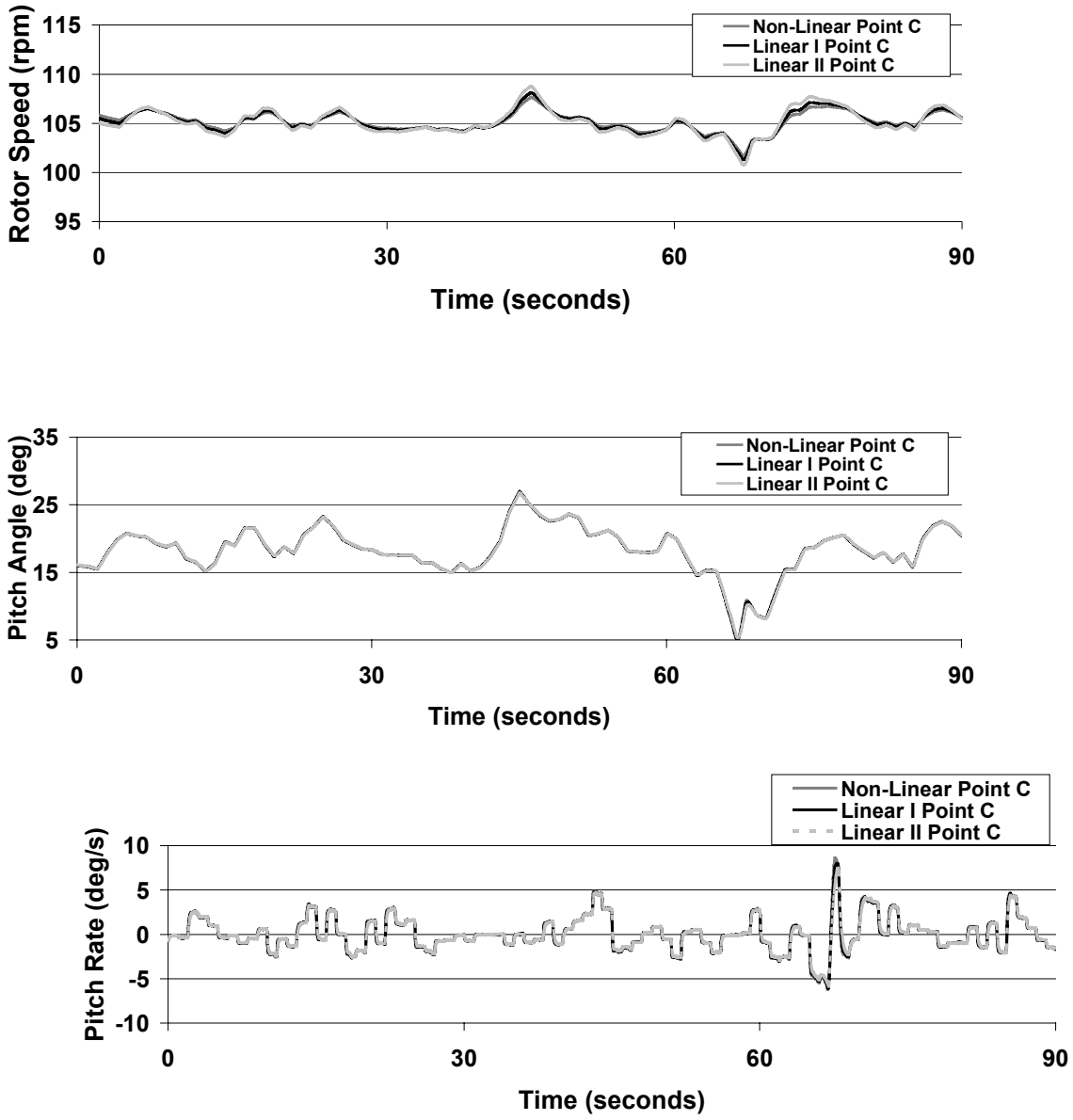

Figure 14. Time-series traces of turbine performance under the optimal gains as determined using each of the three models

Using the gains selected based on the first linear model, the rotor speed nearly duplicates that of the non-linear model optimal gain combination. The pitch rate traces are very similar for all three gain combinations, but the second linear model-based optimal gains slightly out-perform those from the first linear model design. Again, the blade pitch angles commanded by the controller are nearly identical.

Conclusions

This systematic approach to PID-controller design provides a means of visually observing the effect of gain changes on both RMS speed error and actuator duty cycle. While these metrics are in opposition by

nature, the surfaces permit selection of gain values that produce favorable results for both of the metrics. The simplicity of the model requires minimal computation time such that hundreds of simulations can be completed within a few hours. The resolution of the contour plots may easily be improved by increasing the number of simulations. This visualization of the effect of gain permits selection of the best possible combination of controller parameters without requiring a lengthy trial-and-error process.

A valuable aspect of this design approach is the ability to observe the robust nature of the PID controller in this variable-speed wind turbine application. Generation of the surfaces over such varied gain values illustrates the controller sensitivity. The wide, flat surfaces indicate robust behavior. This is valuable information for comparison with other types of controllers.

The non-linear dynamics simulated with this simple model are easily linearized, but several considerations must be made in order to design a PID controller using a linear model. First, the step response that one would expect is drastically different from that observed with the gain combination determined to produce optimum performance. Also, the optimal region based on the balanced performance of the two metrics shifts with the linearization point selection. The surfaces generated by the linear models tend to slope more sharply at the perimeters. These differing slopes yield different areas on the surface that provide the desired combination of the two performance metrics. Operating point selection for a linear model is critical to obtaining the best possible performance from this highly non-linear system.

Although the surfaces are relatively flat, performance does vary when gain combinations from different areas of the surface are compared. These small variations may be exacerbated by more complicated dynamics and sensor noise when these gains are implemented in the field. Thus it is assumed that the non-linear model-based design will be superior to the designs that relied upon the linear model. It is hoped that the choice of controller parameters using the simulation will also be satisfactory for the field turbine.

Lastly, this systematic approach still requires judgment on the part of the designer. A mathematical relationship between the two metrics could eliminate this requirement if such can be found. The systematic design methodology could be automated once weighting functions are determined.

Several opportunities for use of control exist within the wind turbine industry. In addition to speed regulation with mitigated actuator motion, control may be used to extend the fatigue life of blades and rotor shafts. Adding control objectives introduces the need for multiple-input-multiple-output controllers. Also the interaction between control objectives increases the complexity. For instance, blade loads could be affected by the blade-pitch control implemented in this study. To incorporate a blade load objective into a controller, the interaction between the blade pitch motion that regulates the speed and the induced loads must be accommodated within the controller. Fuzzy logic and neural network controllers, as well as state-estimation based controllers, could be employed to incorporate the interaction between the various control objectives.

Nomenclature

J_T Turbine rotor moment of inertia, 1,270 kg•m^2
ω_T Angular shaft speed, rad/s
Q_A Aerodynamic torque, N•m
Q_E Mechanical torque necessary to turn the generator, N•m
ρ Air density, kg/m^3
A Rotor swept area, m^2
R Rotor radius, 5 m
c_q Torque coefficient, dimensionless

λ Blade tip-speed-ratio, dimensionless
β Blade pitch angle, deg
w Wind speed, m/s
P Power extracted from wind, W
c_P Power coefficient, dimensionless
Δ Incremental change
α, δ, γ Linearization coefficients
k_P Proportional gain, deg•s/rad
k_I Integral gain, deg/rad
k_D Derivative gain, deg•s^2/rad

Subscripts
ref Reference point
OP Operating (linearization) point

References

Arsudis, D., and Bohnisch, H. 1990. "Self-tuning linear controller for the blade pitch control of a 100 kW WEC," European Community Wind Energy Conference, H.S. Stephens, Bedford, United Kingdom, Vol. xvi+771, pp. 564-568.

Bongers, P., van Engelen, T., Dijkstra, S., Kock, Z.-J. 1989. "Optimal control of a wind turbine in full load-a case study," Proceedings, European Wind Energy Conference and Exhibition, Peter Peregrinus, London, United Kingdom, Vol. xxx+1063, pp. 345-349.

Bossanyi, E.A. 1989. "Practical results with adaptive control of the MS2 wind turbine," European Wind Energy Conference and Exhibition, Peter Peregrinus, London, United Kingdom, Vol. xxx+1063, pp. 331-335.

De la Salle, S.A., Reardon, D., Leithead, W.E. 1990. "Review of wind turbine control," International Journal of Control, vol. 52, no. 6, pp. 1295-1310.

Ekelund, T. 1994. "Speed control of wind turbines in the stall region." Proceedings, IEEE International Conference on Control and Applications, IEEE; New York, NY, USA, Vol. xlii+1952, pp. 227-32.

Hand, M.M. 1999. "Variable-Speed Wind Turbine Controller Systematic Design Methodology: A Comparison of Non-Linear and Linear Model-Based Designs," NREL/TP-500-25540. Golden, Colorado, USA: National Renewable Energy Laboratory.

Kendall, L., Balas, M.J., Lee, Y.J., and Fingersh, L.J. 1997. "Application of Proportional-Integral and Disturbance Accommodating Control to Variable-speed Variable Pitch Horizontal Axis Wind Turbines," Wind Engineering (12:1); pp. 21-38.
Leithead, W.E., de la Salle, S., Reardon, D., Grimble, M.J. 1991. "Wind turbine modelling and control," International Conference on Control, IEE, London, United Kingdom, Conference Publication No. 332.

Leithead, W.E., de la Salle, S., Reardon, D. 1990. "Wind turbine control objectives and design," European Community Wind Energy Conference, H.S. Stephens, Bedford, United Kingdom, Vol. xvi+771, pp. 510-515.

Stuart, J.G., Wright, A.D., and Butterfield, C. P. 1996. "Considerations for an Integrated Wind Turbine Controls Capability at the National Wind Technology Center: An Aileron Control Case Study for Power Regulation and Load Mitigation," TP-440-21335, National Renewable Energy Laboratory, Golden, CO, USA.

Tangler, J.L. 1987. "User's Guide. A Horizontal Axis Wind Turbine Performance Prediction Code for Personal Computers," Solar Energy Research Institute (now known as National Renewable Energy Laboratory), Golden, Colorado, U.S.A.

REPORT DOCUMENTATION PAGE

Form Approved
OMB NO. 0704-0188

Public reporting burden for this collection of information is estimated to average 1 hour per response, including the time for reviewing instructions, searching existing data sources, gathering and maintaining the data needed, and completing and reviewing the collection of information. Send comments regarding this burden estimate or any other aspect of this collection of information, including suggestions for reducing this burden, to Washington Headquarters Services, Directorate for Information Operations and Reports, 1215 Jefferson Davis Highway, Suite 1204, Arlington, VA 22202-4302, and to the Office of Management and Budget, Paperwork Reduction Project (0704-0188), Washington, DC 20503.

1. AGENCY USE ONLY (Leave blank)	2. REPORT DATE	3. REPORT TYPE AND DATES COVERED
	February 2002	Technical report

4. TITLE AND SUBTITLE
Systematic Controller Design Methodology for Variable-Speed Wind Turbines

5. FUNDING NUMBERS
WER2.4010

6. AUTHOR(S)
M. Maureen Hand and Mark J. Balas

7. PERFORMING ORGANIZATION NAME(S) AND ADDRESS(ES)
National Renewable Energy Laboratory
1617 Cole Blvd.
Golden, CO 80401-3393

8. PERFORMING ORGANIZATION REPORT NUMBER
NREL/TP-500-29415

9. SPONSORING/MONITORING AGENCY NAME(S) AND ADDRESS(ES)
National Renewable Energy Laboratory
1617 Cole Blvd.
Golden, CO 80401-3393

10. SPONSORING/MONITORING AGENCY REPORT NUMBER

11. SUPPLEMENTARY NOTES

NREL Technical Monitor: NA

12a. DISTRIBUTION/AVAILABILITY STATEMENT
National Technical Information Service
U.S. Department of Commerce
5285 Port Royal Road
Springfield, VA 22161

12b. DISTRIBUTION CODE

13. ABSTRACT *(Maximum 200 words)*

Variable-speed, horizontal axis wind turbines use blade-pitch control to meet specified objectives for three operational regions. This paper provides a guide for controller design for the constant power production regime. A simple, rigid, non-linear turbine model was used to systematically perform trade-off studies between two performance metrics. Minimization of both the deviation of the rotor speed from the desired speed and the motion of the actuator is desired. The robust nature of the proportional-integral-derivative controller is illustrated, and optimal operating conditions are determined. Because numerous simulation runs may be completed in a short time, the relationship between the two opposing metrics is easily visualized.

Traditional controller design generally consists of linearizing a model about an operating point. This step was taken for two different operating points, and the systematic design approach was used. The surfaces generated by the systematic design approach using the two linear models are similar to those generated using the non-linear model. The gain values selected using either linear model-based design are similar to those selected using the non-linear model-based design. The linearization point selection does, however, affect the turbine performance. Including complex dynamics in the simulation may exacerbate the small differences evident in this study. Thus, knowing the design variation due to linearization point selection is important.

14. SUBJECT TERMS
Wind turbine; control; variable-speed; PID control; variable pitch

15. NUMBER OF PAGES

16. PRICE CODE

17. SECURITY CLASSIFICATION OF REPORT	18. SECURITY CLASSIFICATION OF THIS PAGE	19. SECURITY CLASSIFICATION OF ABSTRACT	20. LIMITATION OF ABSTRACT
Unclassified	Unclassified	Unclassified	UL